

Two atoms with hyperfine states

April 20, 2023

1 Introduction

We want to explore the effect of hyperfine states (Fig. 1) on the decay rate of the two atoms. Codes associated with calculations are in the [repository](#). We want to address the questions below.

- How to properly describe the hyperfine states?
- Can coherence between different Zeeman sublevel be transferred through the decay?
- How much reduction of the collective effect we can expect by having many branches?
- How different is the functional form of the radiation power at the detector and the functional form of 3P_1 population?

2 Definitions

We consider magnetic sublevel contributions similar to equation (2) in the reference [2]. However, this expression seems to make total decay rate to be dependent on the angular momentum quantum number of the excited state. See `src/Gamma_0_test.jl` to see its dependence. To make total decay rate of a certain level to be F -independent, we add a factor $\sqrt{2F_e + 1}$ to the definition of the atomic rasing operator(equation (2) in [2]).

$$\begin{aligned}\hat{\Sigma}_q &= \sum_{m_g=-F_g}^{F_g} \sqrt{2F_e + 1} (-1)^{F_g - m_g} \begin{pmatrix} F_g & 1 & F_e \\ -m_g & q & m_g - q \end{pmatrix} |F_e m_g - q\rangle \langle F_g m_g| \\ &= \sum_{m_g=-F_g}^{F_g} (-1)^{2m_g - q} |F_g m_g\rangle \langle F_g, m_g; 1, -q| F_e, m_g - q \rangle \langle F_e m_g - q|\end{aligned}$$

The other parts are essentially the same as [2]. As we are considering the cascaded system, we need to consider different transitions. The index l denotes

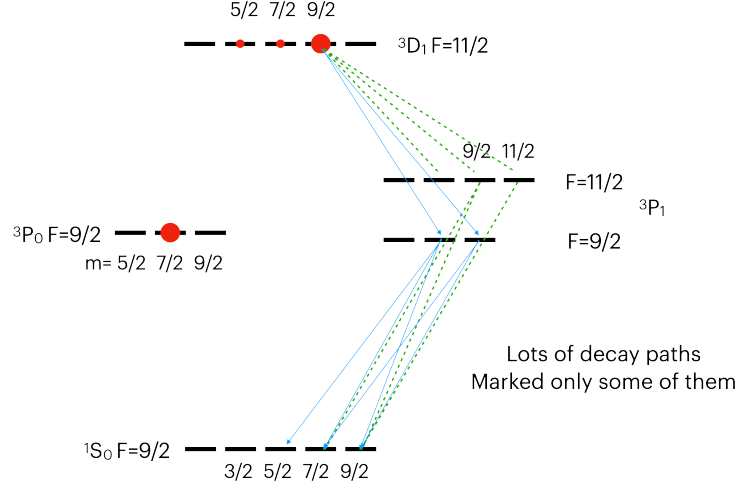


Figure 1: Relevant energy levels of ^{87}Sr atom. Nuclear spin is 9/2. One of the initial population scheme is presented with red blobs. The bigger the blob, the more population.

a specific transition; 1 is for $^3D_1 \rightarrow ^3P_1$, 2 is for $^3D_1 \rightarrow ^3P_0$, and 3 is for $^3P_1 \rightarrow ^1S_0$.

$$\begin{aligned} \mathcal{H} &= \hbar \sum_{l=1}^3 \sum_{i,j=1}^N \sum_{q,q'=-1}^1 J_{ijqq'}^{(l)} \hat{\Sigma}_{iq}^{(l)\dagger} \hat{\Sigma}_{jq'}^{(l)}, \\ \mathcal{L}[\rho] &= \sum_{l=1}^3 \sum_{i,j=1}^N \sum_{q,q'=-1}^1 \frac{\Gamma_{ijqq'}^{(l)}}{2} \left(2\hat{\Sigma}_{jq'}^{(l)} \rho \hat{\Sigma}_{iq}^{(l)\dagger} - \hat{\Sigma}_{iq}^{(l)\dagger} \hat{\Sigma}_{jq'}^{(l)} \rho - \rho \hat{\Sigma}_{iq}^{(l)\dagger} \hat{\Sigma}_{jq'}^{(l)} \right) \\ J_{ijqq'}^{(l)} &= -\frac{3}{4} \Gamma^{(l)} \hat{\mathbf{e}}_q \cdot \text{Re } \mathbf{G}(\mathbf{r}_i, \mathbf{r}_j, \omega_l) \cdot \hat{\mathbf{e}}_{q'}^* \\ \Gamma_{ijqq'}^{(l)} &= \frac{3}{2} \Gamma^{(l)} \hat{\mathbf{e}}_q \cdot \text{Im } \mathbf{G}(\mathbf{r}_i, \mathbf{r}_j, \omega_l) \cdot \hat{\mathbf{e}}_{q'}^* \\ \mathbf{G}(\mathbf{r}, \omega_l) &= \frac{e^{ik_l r}}{k_l^2 r^3} \left[(k_l^2 r^2 + ik_l r - 1) \mathbb{1} + (-k_l^2 r^2 - 3ik_l r + 3) \frac{\mathbf{r} \otimes \mathbf{r}}{r^2} \right] \end{aligned}$$

The intensity of the light at the detector $I(\mathbf{r})$ (from the transition-3) can be calculated as follows:

$$\hat{\mathbf{E}}^+(\mathbf{r}) \propto \sum_{j=1}^N \sum_{q=-1}^1 \mathbf{G}(\mathbf{r}, \mathbf{r}_j, \omega_3) \cdot \hat{\mathbf{e}}_q^* \hat{\Sigma}_{jq}^{(3)}$$

$$I(\mathbf{r}) = \langle \hat{\mathbf{E}}^- \cdot \hat{\mathbf{E}}^+ \rangle$$

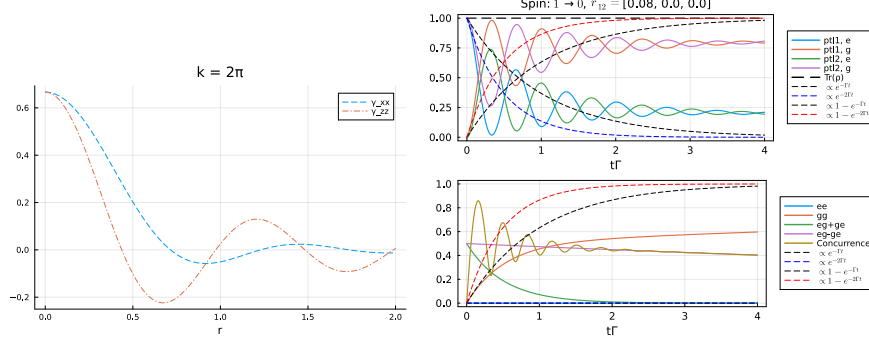


Figure 2: Benchmarking [1]. Left: Green tensor test (Fig. 15.2 of [1]). Right: Concurrence (Fig. 15.5 of [1]) of two atoms separated by $1/12\lambda$ in x direction. The initial Zeeman sublevel is 0 state to make $\cos \theta = 0$, where θ is the angle between two dipoles.

3 Benchmarking

Is my calculation correct? We benchmark the calculation with the results from Ch. 15 of [1]. The reproductions of some of the figures are shown in Fig. 2. For this, we consider only two levels (spin-1 for the excited and spin-0 for the ground) and use the rasing operator to orient the dipoles.

4 Cascaded system

4.1 Can Zeeman sublevel coherence transferred through the decay?

We want to understand whether the coherence among the sublevels can be transferred by the decay. Similar questions are addressed in [3]. As a toy model, we consider a three-level cascaded system of spin 5/2-3/2-1/2. We plot the CG coefficients in Fig. 3

Results are summarized in Fig. 4 and 5. For the system under interest, the first decay channel is 10 times faster than the second decay. Comparing two figures, we can see that g-factor ratio is important for transferring the coherence. If the g-factors are not matched, the coherence is constructively added for some time but then destructively added later.

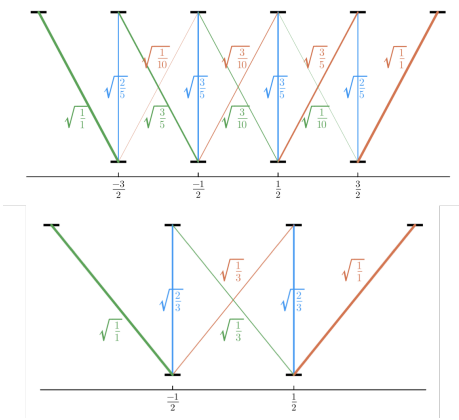
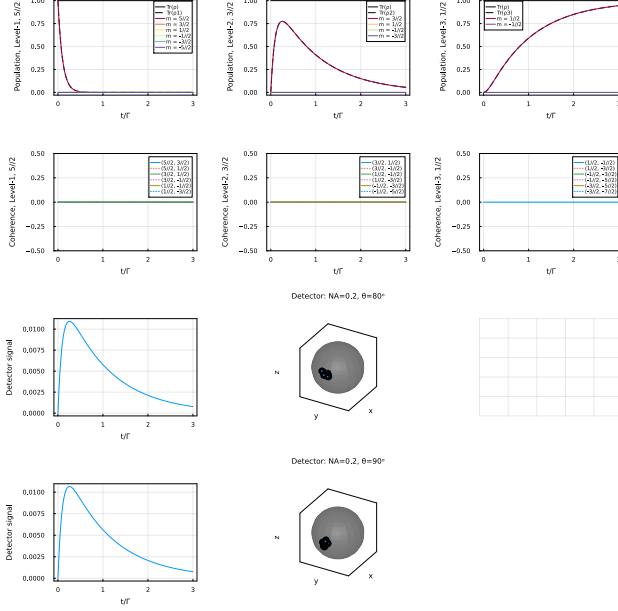
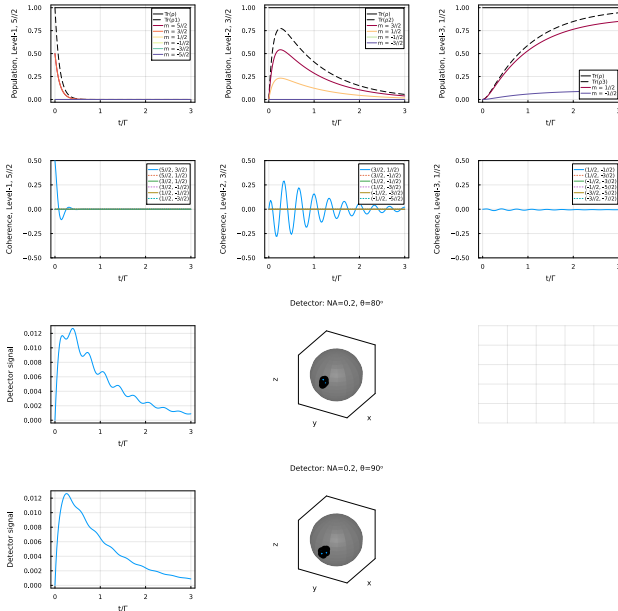


Figure 3: Clebsch-Gordan coefficients of $5/2-3/2$ and $3/2-1/2$.

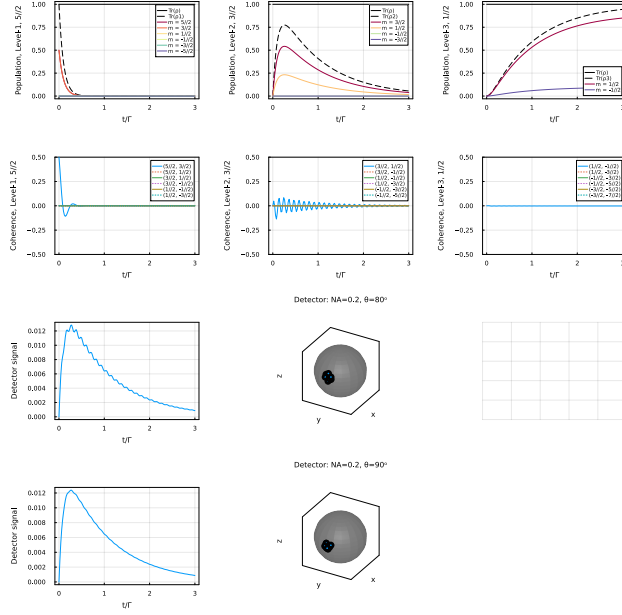


(a) Stretched state as the intial state. First row: diagonal elements of the density matrix. Second row: coherences. Third and forth row: field intensity on the detector. Two slightly different line of sights to emphasize angular dependence of the radiation pattern.

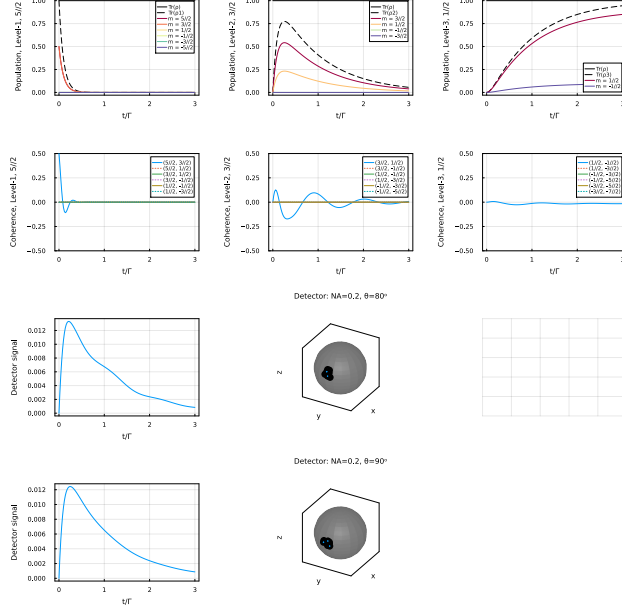


(b) Decay of superposed Zeeman states. Here, g-factors of the two excited states are the same.

Figure 4: Coherence transfer and the Zeeman beat on the detector. The coherence makes radation patterns rotates. The populations of the sublevels does not oscillate.



(a) When intermediate state has 3 times larger g-factor.



(b) When intermediate state has 3 times lower g-factor.

Figure 5: Different g-factors and the amount of coherence transferred.

If we increase the strength of the magnetic field, the number constructive-destructive transfer cycles increases (as they follows the Lamor frequencies). Therefore, it becomes more sensitive to the g-factor mismatch. If we can apply a very strong magnetic field, that is, the Lamor frequencies are much higher than the decay rates, we can neglect this Zeeman beat effect as there is no coherence between sublevels of 3P_1 manifold. Due to the technical limitation of the current setup, we decided to go very low field; we reduce the rotating speed of the radiation pattern much lower than the decay rate.

This idea may be applied to the many particle coherence and it seems more nature for those cases. If we have a strong coherence built through the superradiance of the first decay path, we are very likely to have a strong coherence on the second decay path. But the wavelengths of two decay channels are very different.

4.2 Sublevel and the collective effect

Now we explore collective effect with two atoms and four levels to mimic our real atom and explore some effect of the sublevel branching. First we look at the case that two atoms are at a point. We expect the largest collective effect for this case. The results are summarized in Fig. 6. We see a quite strong starting Zeeman sublevel dependence on the fitted lifetime.

Figure 7 present similar plots with $3 \mu\text{m}$ (along x) separated atoms. It is much stable and fitting almost correct values but we can find relative difference between two different initial sublevels.

4.3 Radiation pattern and the population

We explore radiation pattern of the atoms and how it is different from the atomic populations. Figure 8 shows an example of the radiation pattern.

The difference between the population and the radiated power is shown in Fig. 9 and 10. To understand what is happening, we consider two atoms at a point with different Zeeman sublevels.

5 Hyperfine branching ratio

Here, we leave a note on branching ratio calculation for D-P decay paths. From [4], equation (7.283), the reduced dipole moment of the transition between two different fine structure states are given by

$$\begin{aligned} \langle J || \mathbf{d} || J' \rangle &\equiv \langle LSJ || \mathbf{d} || L'SJ' \rangle \\ &= \langle L || \mathbf{d} || L' \rangle (-1)^{J'+L+1+S} \sqrt{(2J'+1)(2L+1)} \left\{ \begin{array}{ccc} L & L' & 1 \\ J' & J & S \end{array} \right\} \end{aligned}$$

Here, (un)primed numbers are for the (excited)ground states. For $^3D_1 \rightarrow ^3P_{J'}$, where $J' \in (0, 1, 2)$ and $J = 1, L = 2, L' = 1, S = 1$ are fixed. The ratio

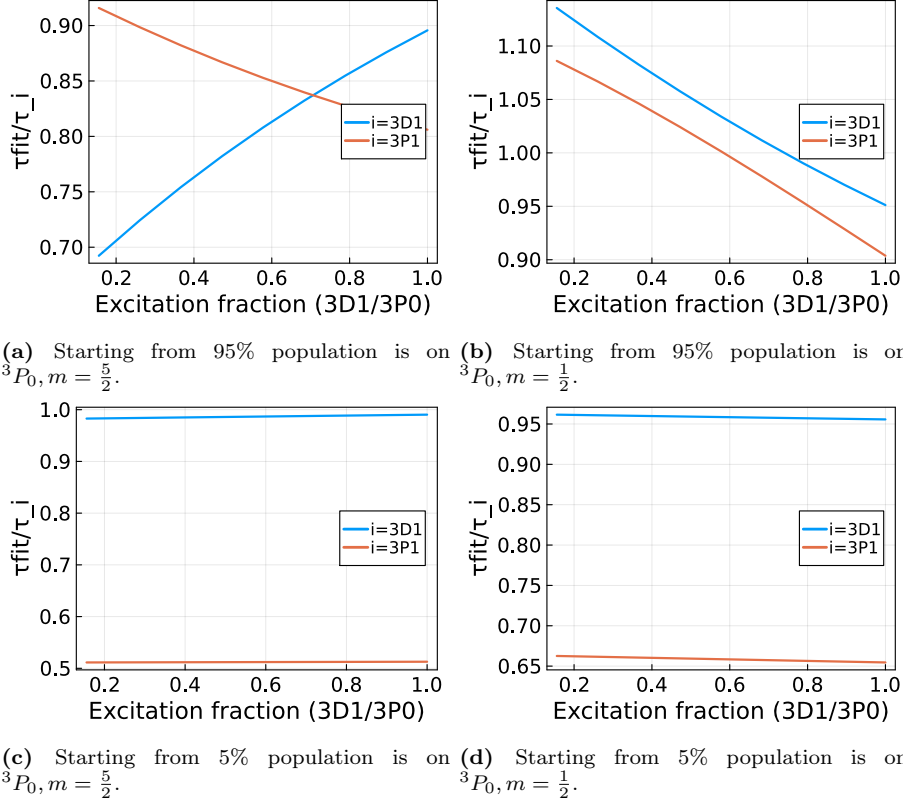


Figure 6: Initial condition dependence of the lifetime. We plot the ratio between input single particle decay rate and the double-exp fitted lifetime assuming the detector signal is proportional to the population. We vary the intial Zeeman sublevel and the excitation fraction between 3D_1 and 3P_0 .

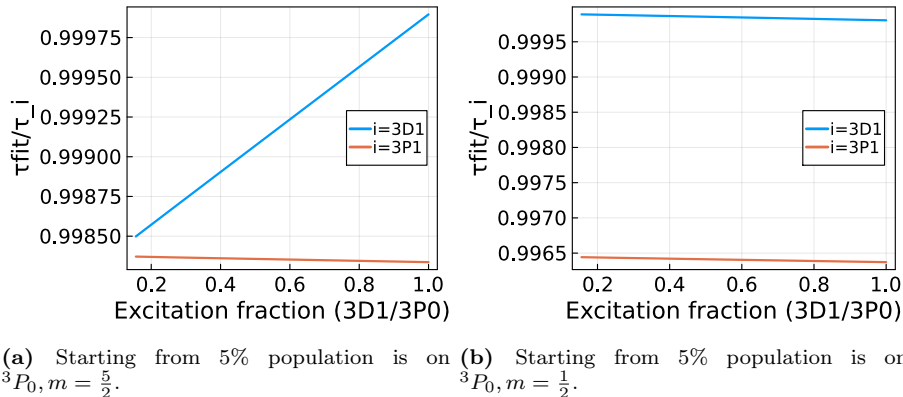


Figure 7: Similar to Fig. 6 but with atoms apart 3 μm along x -axis.

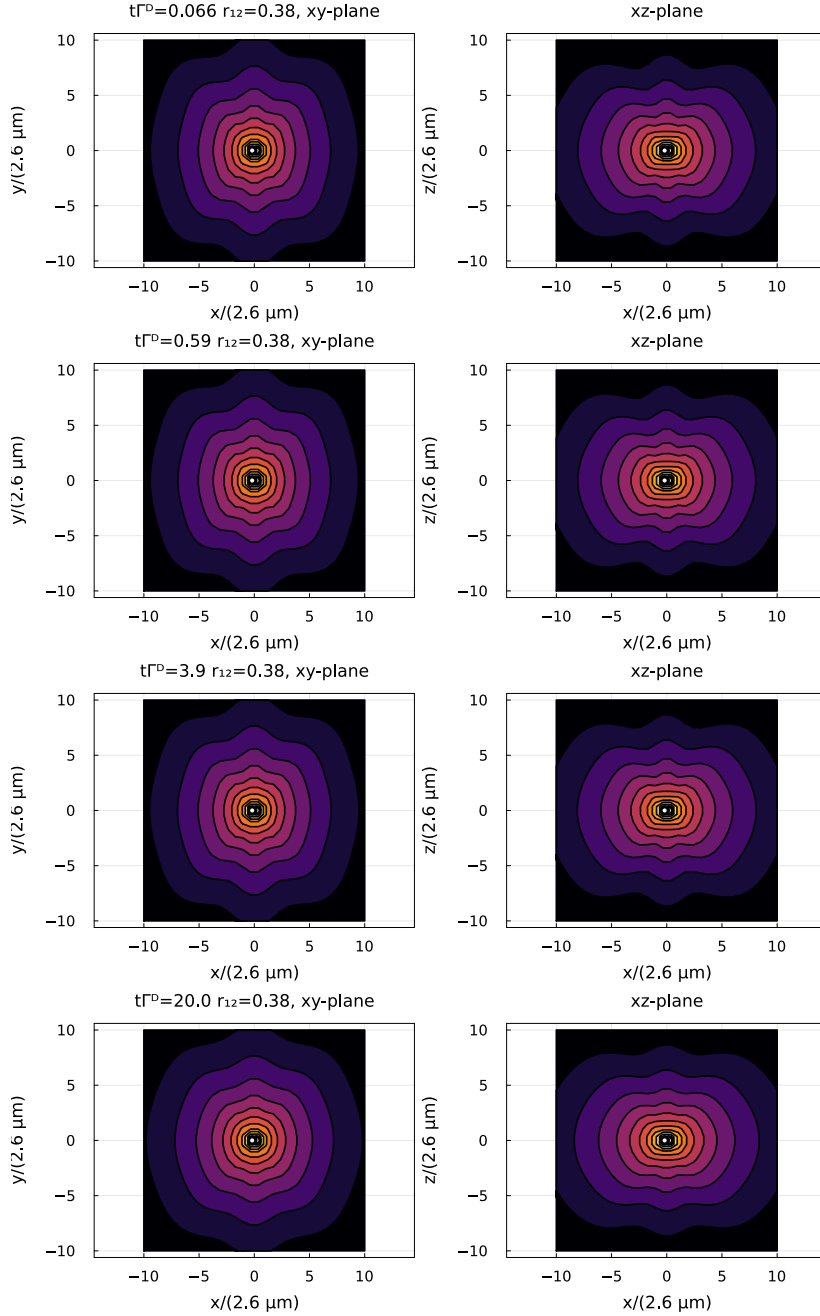


Figure 8: Radiation pattern of two atoms separated by $1 \mu\text{m}$ along x -axis. For the visibility, we plot log-intensity's spatial cross sections. Each row represent different time section, denoted as a unit of 3D_1 state's lifetime (Γ^D). The initial sublevel is $1/2$.

and we neglect the magnetic field. At later time, the modulation of the radiation pattern gets smoother, which implies that we directionality of the collective effect.

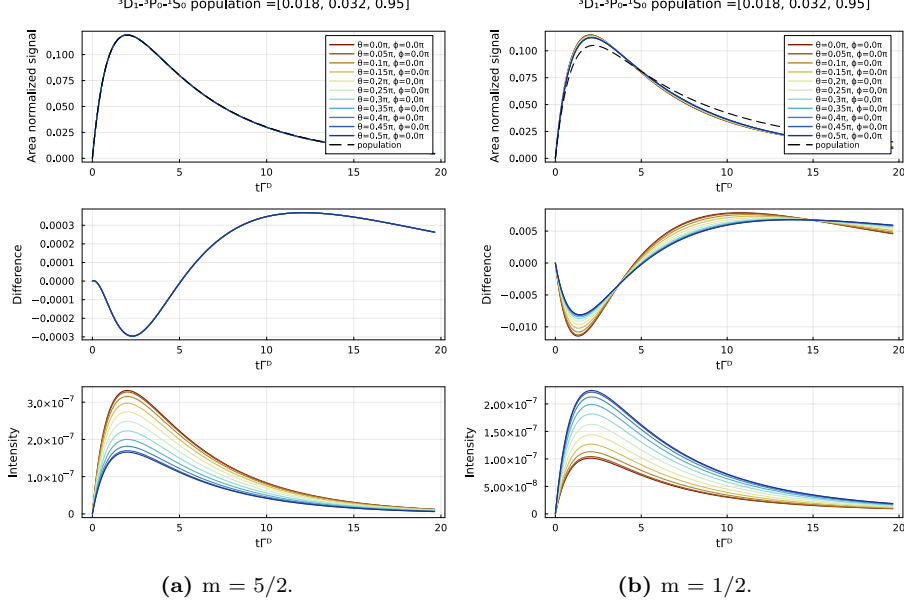


Figure 9: Difference between the population and the radiated power. θ denotes the polar angle of the detector. Top row represents the intensity of the radiation power for the comparison, the intensity is normalized by its own. Bare intensity is plotted at the bottom row. The center row shows the difference between the normalized radiation intensity and the population.

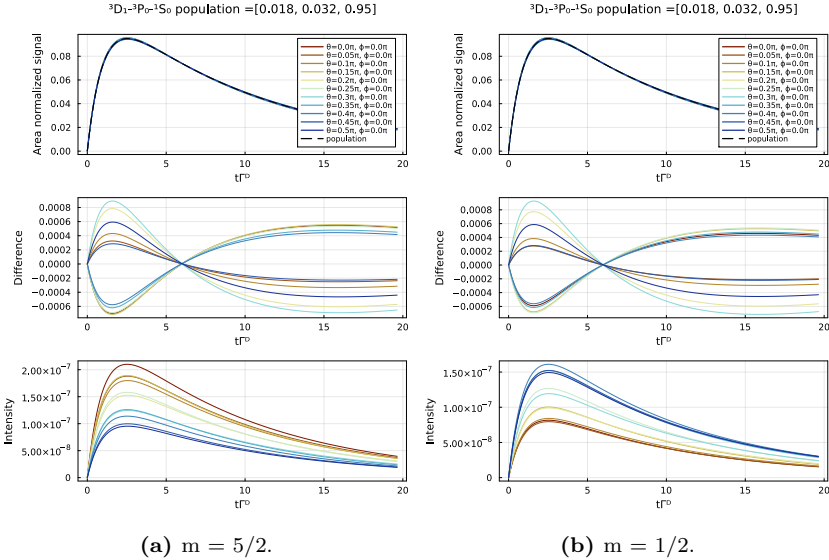


Figure 10: Similar to Fig. 9, but with $3\mu\text{m}$ separation along x-axis. We can see at most percent level deviation from the population.

between squared dipole matrix elements of different ${}^3P_{J'}$ states will be

$$|\langle {}^3D_1 || \mathbf{d} || {}^3P_{J'} \rangle|^2 \propto (2J' + 1)(2 \cdot 2 + 1) \left| \left\{ \begin{array}{ccc} 2 & 1 & 1 \\ J' & 1 & 1 \end{array} \right\} \right|^2$$

This gives the ratio $\frac{5}{9} : \frac{5}{12} : \frac{1}{36}$. The actual decay rate will depends on the frequency of the transition. For the decay rate Γ from e to g ,

$$\Gamma = \frac{\omega_0^3}{3\pi\epsilon_0\hbar c^3} |\langle g | \mathbf{d} | e \rangle|^2.$$

The decay rate will be proportional to the cube of the frequency or the inverse cube of the wavelength. The transition wavelengths of ${}^3P_{J'}$ are (2.60315, 2.7362, 3.06701) μm . The actual decay ratio will be

$$\frac{5}{9} \frac{1}{2.6^3} : \frac{5}{12} \frac{1}{2.74^3} : \frac{1}{36} \frac{1}{3.07^3} = 0.597 : 0.385 : 0.018$$

We now consider the hyperfine structure. The matrix element has the same form as before.

$$\begin{aligned} \langle F || \mathbf{d} || F' \rangle &\equiv \langle JIF || \mathbf{d} || J'IF' \rangle \\ &= \langle J || \mathbf{d} || J' \rangle (-1)^{F'+J+1+I} \sqrt{(2F'+1)(2J+1)} \left\{ \begin{array}{ccc} J & J' & 1 \\ F' & F & I \end{array} \right\} \\ &= \langle L || \mathbf{d} || L' \rangle (-1)^{J'+L+1+S} \sqrt{(2J'+1)(2L+1)} \left\{ \begin{array}{ccc} L & L' & 1 \\ J' & J & S \end{array} \right\} \\ &\quad \times (-1)^{F'+J+1+I} \sqrt{(2F'+1)(2J+1)} \left\{ \begin{array}{ccc} J & J' & 1 \\ F' & F & I \end{array} \right\}. \end{aligned}$$

$$\begin{aligned} |\langle {}^3D_1, F || \mathbf{d} || {}^3P_{J'}, F' \rangle|^2 &= (2J'+1)(2 \cdot 2 + 1)(2F'+1)(2 \cdot 1 + 1) \\ &\quad \times \left| \left\{ \begin{array}{ccc} 2 & 1 & 1 \\ J' & 1 & 1 \end{array} \right\} \left\{ \begin{array}{ccc} 1 & J' & 1 \\ F' & F & 9/2 \end{array} \right\} \right|^2 |\langle L=2 || \mathbf{d} || L'=1 \rangle|^2 \end{aligned}$$

The results are shown in Fig. 11.

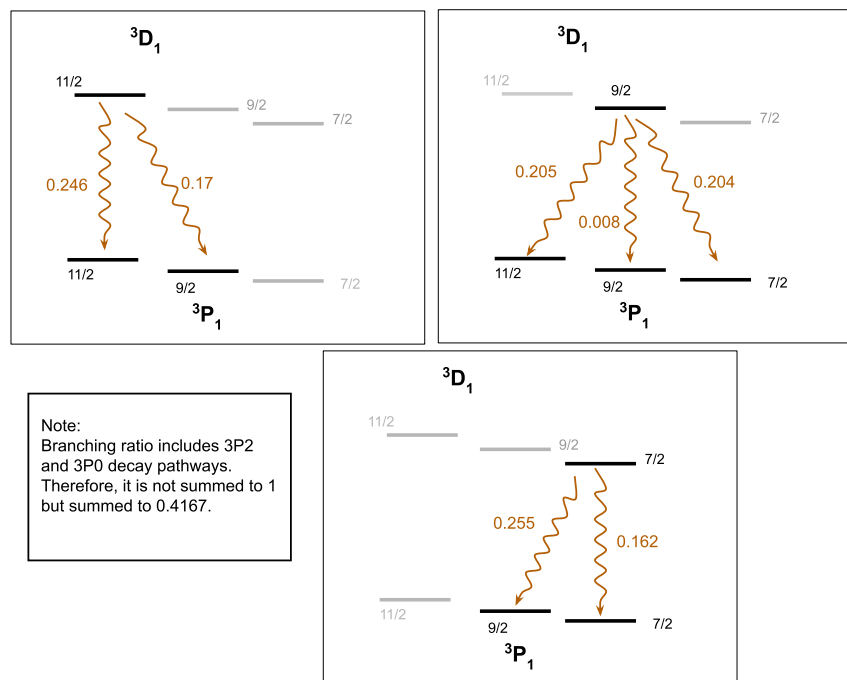


Figure 11: Branching ratio for $|{}^3D_1, F\rangle \rightarrow |{}^3P_1, F'\rangle$

References

- [1] G. S Agarwal. *Quantum optics*. Cambridge University Press, Cambridge, 2012. OCLC: 817224926.
- [2] Ana Asenjo-Garcia, H. J. Kimble, and Darrick E. Chang. Optical waveguiding by atomic entanglement in multilevel atom arrays. *Proceedings of the National Academy of Sciences*, 116(51):25503–25511, December 2019.
- [3] B J Dalton. Theory of cascade effects on quantum beats. *Journal of Physics B: Atomic and Molecular Physics*, 12(16):2625–2636, August 1979.
- [4] Daniel A Steck. *Quantum and Atom Optics*. 2022.